Original Article

Soft substrates direct stem cell differentiation into the chondrogenic lineage without the use of growth factors

Journal of Tissue Engineering
Volume 13: 1–19

DOI: 10.1177/20417314221122121
journals.sagepub.com/home/tej
SAGE

Tosca Roncada[1], Roxane Bonithon[2], Gordon Blunn[1] and Marta Roldo[1]

Abstract

Mesenchymal stem cells (MSCs) hold great promise for the treatment of cartilage related injuries. However, selectively promoting stem cell differentiation *in vivo* is still challenging. Chondrogenic differentiation of MSCs usually requires the use of growth factors that lead to the overexpression of hypertrophic markers. In this study, for the first time the effect of stiffness on MSC differentiation has been tested without the use of growth factors. Three-dimensional collagen and alginate scaffolds were developed and characterised. Stiffness significantly affected gene expression and ECM deposition. While, all hydrogels supported chondrogenic differentiation and allowed deposition of collagen type II and aggrecan, the 5.75 kPa hydrogel showed limited production of collagen type I compared to the other two formulations. These findings demonstrated for the first time that stiffness can guide MSCs differentiation without the use of growth factors within a tissue engineering scaffold suitable for the treatment of cartilage defects.

Keywords

Alginate, cartilage regeneration, hydrogels, mechanobiology, stiffness

Date received: 6 June 2022; accepted: 3 August 2022

Introduction

Osteochondral defects are lesions that involve both the articular cartilage and the underlying subchondral bone and can be caused by ageing, disease (e.g. osteoarthritis) or traumatic injuries.[1,2] Trauma associated osteochondral injuries frequently occur in active young patients and if left untreated will lead to the development of osteoarthritis.[3,4] Due to its avascular nature, the poor diffusion of nutrients and the lack of abundant progenitor cells, cartilage has a limited ability to self-repair.[5] Currently, several clinical treatments are available, such as marrow stimulation, autologous chondrocyte implantation and osteochondral autograft and allograft, but none of them has achieved the complete healing of the osteochondral lesion.[6–10] In the last two decades, research has been focusing on tissue engineering (TE) as a possible tool for osteochondral regeneration. Mesenchymal stem cells (MSCs) are amongst the most promising cells for TE applications, they are non-haematopoietic multipotent stem cells with self-renewal properties and the ability to differentiate into a variety of mesenchymal tissue types such as osteogenic, chondrogenic and adipogenic.[11,12] They represent a promising alternative to the currently used articular chondrocytes, as a larger number of cells can be obtained from a wider variety of sources such as bone marrow, peripheral blood, adipose tissue, dental pulp, placenta or the umbilical cord.[13] Overall, cartilage development is a tightly regulated process, difficult to recapitulate both in vitro and in vivo. In order to accelerate matrix production by implanted MSCs and improve matrix quality it is important to ensure stem cells differentiate into chondrocytes.[2] Chondrogenic induction

[1]School of Pharmacy and Biomedical Sciences, University of Portsmouth, Portsmouth, UK
[2]School of Mechanical and Design Engineering, University of Portsmouth, Portsmouth, UK

Corresponding author:
Marta Roldo, School of Pharmacy and Biomedical Sciences, University of Portsmouth, White Swan Road, Portsmouth, PO1 2DT, UK.
Email: marta.roldo@port.ac.uk

of MSCs in vitro usually requires the use of growth factors such as transforming growth factor beta (TGF-β), however, their clinical application is still limited as undesired off-target effects on the synthesis and functionality of cartilage matrix components have been shown.[14] Mueller et al. showed that both TGF-β1 and TGF-β3 induce hypertrophy of MSCs.[15] A recent study revealed that genes associated with cartilage hypertrophy were upregulated in MSCs after a single day of exposure to TGF-β1, and their expression remained elevated even after its removal.[16] For MSC-based tissue engineering of articular cartilage, the expression of hypertrophy markers is a major concern because hypertrophy will ultimately potentially lead to apoptosis, vascular invasion, and cartilage mineralisation.[17] Thus, alternative strategies to differentiate MSC into chondrocytes are required. Recent studies have shown that directing stem cell fate could be achieved by finely tuning the mechanical environment.[18–24] In particular, stiffness, defined as the extent to which a material resists deformation in response to an applied force, has been shown to influence cell phenotype and to play a pivotal role in tissue development, homoeostasis and disease.[25–30] On stiff substrates, MSCs have been shown to acquire an elongated spindle shape triggering the activation of extracellular signal-regulated kinase 1 (*ERK1*) and *ERK2* thus promoting osteogenic differentiation.[31,32] Conversely, several studies demonstrated that soft hydrogels (0.1–15 kPa stiffness), significantly upregulate chondrogenic markers and matrix deposition.[21,33–36] A recent study not only demonstrated that soft hydrogels (2 kPa) supported higher cell viability compared to stiffer hydrogels (60 kPa), but they also exhibited increased expression of aggrecan and collagen type II.[37] Even though soft substrates do not mimic the stiffness of native cartilage, they appear to simulate the mechanical properties of the developing limb bud, suggesting that developing soft substrates simulating the mechanical properties of cartilage development could represent a promising strategy for directing MSCs into chondrocytes.[21,38] However, all studies to date have been conducted in the presence of chondrogenic media containing TGF-β thus making it difficult to understand whether stiffness alone could drive the differentiation of MSCs down the chondrogenic lineage. In the present study, collagen and alginate hydrogels with different stiffness were developed to evaluate whether or not stiffness alone could drive the differentiation of MSCs into chondrocytes. We hypothesise that controlling the stiffness of the scaffold successful differentiation of MSCs down the chondrogenic lineage can be obtained in the absence of growth factors.

Materials and methods

Materials

Collagen from calf skin, glacial acetic acid (⩾99%), sodium hydroxide ⩾97.0% pellets, bovine serum albumin, alginic acid sodium salt from brown algae low viscosity, Ficoll Histopaque®-1077 (1.077 g/mL), Alcian Blue 8XG solution, Alizarin Red S, Oil Red O, calcium chloride anhydrous ⩾96.0%, paraformaldehyde (PFA) powder were purchased from Merck Life Science UK Limited (Gillingham, UK). Crystalline sucrose, DMEM (high glucose), GlutaMAX™ Supplement, foetal bovine serum (FBS), Hank's Balanced Salt Solution (HBSS), Gibco™ phosphate buffered saline (PBS, pH 7.4), Gibco™ trypsin-EDTA (0.25%), phenol red, Gibco™ penicillin-streptomycin (10,000 U/mL), Gibco™ StemPro™ chondrogenesis differentiation Kit, Gibco™ StemPro™ osteogenesis differentiation Kit, Gibco™ StemPro™ adipogenesis differentiation Kit, Invitrogen™ Ethidium Homodimer-1 (EthD-1), Invitrogen™ Calcein, AM, cell-permeant dye phalloidin Dylight 550, Invitrogen™ CellTrace™ CFSE Cell Proliferation Kit for flow cytometry, Molecular Probes™ PrestoBlue™ Cell Viability Reagent, Invitrogen™ 2-NBDG (2-(N-(7-Nitrobenz-2-oxa-1,3-diazol-4-yl)Amino)-2-Deoxyglucose), epredia 125 ML OCT embedding cryoembedding matrix, Anti-Mouse IgG (whole molecule) F(ab′)2 fragment–FITC, Invitrogen™ DAPI (4′,6-Diamidino-2-Phenylindole, Dihydrochloride), Epredia™ SuperFrostTM microscope slides, ground 90°, 2-methylbutane (isopentane) 99 + % extra dry, AcroSeal™, Fisherbrand™ RNase-Free disposable pellet pestles, Applied Biosystems™ High-Capacity cDNA Reverse Transcription Kit with RNase Inhibitor were purchased from Fisher Scientific (Loughborough, UK). Mouse anti sheep CD44 antibody clone 25.32, Mouse anti sheep CD45 antibody clone 1.11.32, SsoAdvanced Universal SYBR Green Supermix were purchased from Biorad (Watford, UK). Purified anti-human CD29 antibody was purchased from Biolegend (London, UK). PE Mouse Anti-Human CD34 was purchased from BD Biosciences (Wokingham, UK). Anti-Aggrecan antibody [6-B-4], Anti-Collagen II antibody, Rabbit monoclonal [EPR7785] to Collagen I, Goat Anti-Rabbit IgG H&L (Alexa Fluor® 594) were purchased from Abcam (Cambridge, UK). RNeasy Micro Kit, QIAzol Lysis Reagent, QIAshredder were purchased from Qiagen (Manchester, UK) RTqPCR specific primers were purchased from Eurofins Genomics (Ebersberg, Germany).

Gel formulation and analysis

Collagen alginate (col/alg) hydrogel preparation. Alginate is a natural polymer commonly used in tissue engineering of cartilaginous tissues as it has been shown to promote the typical chondrogenic phenotype with rounded morphology and collagen type II and proteoglycans synthesis.[39–43] Alginate undergoes rapid and gentle gelation through the interaction with divalent cations, which makes it attractive for cell encapsulation. Furthermore, its mechanical properties can be easily tuned by increasing the concentration of the crosslinker.[39,42,44] However, alginate lacks bioactive ligands essential for cells anchoring, which limits cells adhesion

and proliferation. Therefore, alginate was combined with collagen type I. Collagen type I has been extensively used in tissue engineering as it represents the most abundant protein of the body and it has excellent biocompatibility, good biodegradability, and weak antigenicity.[5,45–48]

A 1% w/v collagen solution was prepared by dissolving type I collagen powder from calfskin in acetic acid (2% v/v) at 4°C overnight. Once dissolved, the pH of the collagen solutions was adjusted to 7.4 by the addition of 1 N NaOH. DMEM was added to further dilute the collagen solution to 0.5%. A 5% w/v alginate solution was prepared by dissolving alginic acid sodium salt powder in a sterile calcium-free phosphate buffer solution (PBS 1X, pH = 7.4). The solution was then slowly stirred until fully dispersed, to obtain a viscous solution. Alginate and collagen solutions were then mixed in a 1:1 ratio. Hydrogels were first crosslinked by calcium diffusion through the gel by using different concentrations of $CaCl_2$ (30–100 mM). To form bulk hydrogels for rheological analysis 1 mL of col/alg solution was added to a $CaCl_2$ bath in a 6 well plate. For cellular studies 50 µL of col/alg mixture were added to a $CaCl_2$ bath in a 24 well plate. A ratio of col/alg mixture and $CaCl_2$ of 1:5 was used for both bulk and beads formation. Hydrogels were then placed for 3 h at 37°C in an incubator to complete collagen gelation.

Rheological analysis. Rheological characterisation was performed using a Rotational Rheometer (TA Discovery HR 10 TA Instruments, Wilmslow, United Kingdom) with a 40 mm diameter stainless steel flat plate. A strain sweep of fully formed hydrogels (1 mL) was performed in the 0.1%–100% strain range at a frequency of $\omega_0 = 1.0$ Hz (6.3 rad s^{-1}) in order to determine the linear- viscoelastic regime (LVE) which was then used for the frequency sweep tests. Frequency sweep tests were performed to study how the elastic modulus (G′) and viscous modulus (G″) changed with frequency. Frequency sweeps from 0.01 to 100 Hz were conducted at the LVE strain amplitude determined in the strain sweeps tests. Each hydrogel sample was used for only one test and all tests were conducted in triplicate at 37°C. Data were analysed using TRIOS software (TA Instruments, Wilmslow, United Kingdom). The Young's modulus was calculated using equation (1):

$$E = 2 \times G \times (1 + v) \quad (1)$$

where E is Young's modulus, G is the complex modulus, and $v = 0.5$ is the Poisson's Ratio.[49–51]

Porosity measurements. The porosity and pore diameter were examined on freeze-dried hydrogels ($n = 3$) using high-resolution X-ray computed tomography (XCT, Versa 520, Zeiss, Pleasanton, US). The images were collected at 30 kV and 2 W with an isotropic voxel size of 6.36 µm, 2401 projections were collected over 360° with an exposure time of 1.5 s per projection. The 3D data was then analysed with Avizo (9.7.0, ThermoFisher Scientific, Waltham, US). After reconstruction, a volume of interest was extracted containing only the sample in the field of view (~$9.5 \times 9.5 \times 1.5$ mm^3) and converted to a binary image using an interactive threshold method. From the segmented images, the diameter of the pores and the porosity of the sample were calculated. Outliners pores (i.e. diameter exceeding 250 µm) at the edges of the samples were excluded from the analysis.

Hydrogels degradation. Freeze-dried hydrogels were weighed and placed in 1 mL of phosphate buffer solution (PBS, pH = 7.4) at 37°C in a shaking incubator (rpm 150). The PBS was changed every 2 days. At 7 and 14 days, the hydrogels were removed from the buffer, freeze-dried and weighed. The extent of *in vitro* degradation was calculated using equation (2):

$$Weight\ loss(\%) = \left[(W_i - W_d) / W_i \right] \times 100 \quad (2)$$

where W_i is the initial weight of the scaffold and W_d is the weight of the scaffold after the degradation experiment. The surface of freeze-dried samples was evaluated by scanning electron microscopy (30 kV, SEM, EVO MA10, White Plains, US) on day 0, 7 and 14 of the degradation studies. Images were taken by a scanning electron microscope, after having sputter coated the samples with gold and palladium (Polaron e500, Quoram Technologies, Lewes UK). Experiments were done in triplicate.

Ovine bone marrow mesenchymal stem cells (oMSCs) isolation and characterisation

oMSCs isolation. Bone marrow from iliac crest was aspirated from five sheep. All procedures were carried out in accordance with the UKs Animals (Scientific procedures) Act 1986 at the Royal Veterinary college, North Mymms. The project was approved by the animal welfare and ethical review body of the Royal Veterinary College and the procedures were carried out under a Home Office Project (project licence number P16F4AA0A). Home office personal licences were held by all those taking part in any surgical procedure. Anaesthetised sheep were positioned in sternal recumbency and the skin over the iliac crest prepared by shaving followed by treating with povidone iodine solution. Under aseptic conditions stab incision was made and the cancellous bone was accessed using a Jamshid needle. A 10 mL syringe pre-loaded with 1 mL of heparin at 1000 iu/mL was used to aspirate 5 mL of bone marrow from the intramedullary cavity of the iliac crest. The bone marrow was then transferred into a sterile universal tube, swirled slightly to mix the heparin with marrow to prevent clotting and a buffy layer coating nucleated cells was separated from red blood cells using Ficoll-Paque (1.077 g/mL).

Firstly, a layer of Ficoll was added into a tube, then the aspirate was gently dispensed into the tube in order to obtain an upper layer of bone marrow and a bottom layer of Ficoll. Subsequently, the samples were centrifuged at 300 *g* (Eppendorf® Centrifuge 5702, Eppendorf UK LTD, Stevenage, UK) for 25 min, leaving a buffy layer at the interface between a Ficoll-erythrocyte residue at the bottom and a plasma layer above. The buffy layer was washed in sterile PBS and centrifuged at 300 *g* for 5 min. The pellet was resuspended in DMEM supplemented with 10% foetal bovine serum (FBS), penicillin/streptomycin (1%) and plated into a 25 cm^2 flask. Cells were cultured in a humidified atmosphere at 37°C, 5% CO_2 and at 80% confluence, cells were trypsinized and expanded. oMSCs were characterised at passage 3 and all experiments described below were performed at passage 4, and for each experiment cells derived from three different animals were employed and all cell samples were tested in triplicate.

Flow cytometric analysis. At passage 3, cells were analysed for expression of surface marker molecules by direct immunofluorescent staining. Briefly, cell pellets were resuspended in PBS, and incubated with fluorescein isothiocyanate (FITC)– or phycoerythrin (PE)–conjugated antibodies: CD44-FITC (1:25), CD45-FITC (1:50), mouse anti-human CD34-PE (1:10), and CD29-PE (1:10) for 1 h at room temperature. Antibody-treated cells were washed with PBS and spun down (300 *g*). For each sample, the cell pellet was resuspended in 500 µL of PBS and 10,000 events per assays were collected using the FACSCalibur (BD Biosciences, Wokingham, UK) and analysed using CellQuest software (BD Biosciences, Wokingham, UK). Unstained oMSC were used as control. See Supplemental Figure 5 for gating strategy.

Multipotential characterisation of oMSCs

Adipogenic differentiation. oMSCs were seeded at 30,000 cells/cm^2 in a 24 well plate. Adipogenesis was induced by culture for 21 days in StemPro™ Adipogenesis Differentiation Kit (supplemented with 0.1 mM dexamethasone, 50 mM indomethacin, 0.45 mM 3-isobutyl-1-methylxanthine (IBM)X and 10 mg/mL Insulin.). Adipogenic differentiation was compared to a control consisting of cells cultured for the same period of time in 10% FBS/DMEM. The cells were grown at 37°C, 5% CO_2 and the presence of lipid droplets within the cells was confirmed by staining with Oil Red O on day 21. Briefly, an Oil Red O stock solution was prepared by dissolving 0.5 g of Oil Red O powder in 100 mL of isopropanol. An Oil Red O working solution was prepared fresh each time by diluting it 3:2 with deionised water. On day 21 oMSCs were fixed with 500 µL PFA 4% in PBS for 10 min and washed three times with PBS. oMSCs were then rinsed with 60% isopropanol and then stained with 500 µL Oil Red O working solution for 15 min. oMSCs were then rinsed in PBS and imaged using an inverted microscope connected to a camera (Axio Vert A1, Zeiss White Plains, US).

Osteogenic differentiation. oMSCs were seeded at 30,000 cells/cm^2 in a 24 well plate. Osteogenesis was induced by culture for 21 days in StemPro™ Osteogenesis Differentiation Kit (Gibco) (supplemented with 100 nM dexamethasone, 50 µg/mL L-ascorbic acid 2-phosphate and 10 mM beta-glycerophosphate), according to the manufacturer's instructions. Osteogenic differentiation was compared to a control consisting of cells cultured for the same period of time in 10% FBS/DMEM. Differentiation was confirmed by Alizarin S Red staining. Alizarin Red S staining was prepared by dissolving 0.492 g of Alizarin Red S powder into 50 mL of deionised water. On day 21 oMSCs were fixed in 500 µL of methanol for 10 min and washed three times with PBS. oMSCs were stained with Alizarin Red S staining (pH 4.2) for 15 min at room temperature. oMSCs were then rinsed five times with deionised water and imaged using an inverted microscope connected to a camera.

Chondrogenic differentiation. Chondrogenesis was assessed using the micropellet formation (2.5×10^5 cells) technique. oMSCs pellet was cultured in StemPro™ Chondrogenesis Differentiation Kit (1x ITS, 40 µg/mL proline, 100 nM dexamethasone, 100 µm ascorbate-2-phosphate and 10 ng/mL TGF-β) for 21 days in a 24 well plate, according to manufacturer's instructions. Chondrogenic differentiation was compared with cell micropellets cultured for the same period of time with 10% FBS/DMEM. Differentiation was confirmed by Alcian blue staining. On day 21 oMSCs were fixed with 500 µL PFA 4% for 1 h and washed three times with PBS. The pellets were then stained overnight in 1% Alcian blue solution. The pellets were then washed extensively with PBS 1X and then imaged using an inverted microscope connected to a camera.

Hydrogel cytocompatibility

Cell encapsulation. oMSCs (passage 4) were incubated with trypsin-EDTA for 5 min, centrifuged, and resuspended in 1 mL of DMEM supplemented with 10% (v/v) FBS and counted using a haemocytometer. A dilution of 1×10^6 cells/mL was used for each experiment and hydrogels of 50 µL containing 50,000 cells were used in each experiment. Briefly 1×10^6 cells were pelleted by centrifugation and the supernatant was removed in order not to dilute the 1 mL col/alg solution that was subsequently added and mixed gently to avoid bubble formation. Col/alg hydrogels were formed by adding dropwise 50 µL of the mixture to a $CaCl_2$ bath and allowed to gel for 10 min. Then the hydrogels with cells were placed at 37°C in an incubator for 3 h and 1 mL of DMEM supplemented with 10% (v/v) FBS was subsequently added.

Live/dead staining. Viability of oMSCs encapsulated into the hydrogels was analysed at day 1 and 7 by double staining with ethidium homodimer-1 and calcein-AM assay according to the manufacturer's instructions. Briefly, cells were washed with PBS 1X and stained with 500 µL of calcein-AM 2 µM and ethidium homodimer-1 4 µM for 2 h at 37°C. Then samples were rinsed twice with PBS 1X and imaged with a confocal laser scanning microscope (LSM 880, Zeiss, Oberkochen, Germany) at 488 and 543 nm. Cell viability was quantified using Image-J software (National Instruments, Austin, US). Viability data were calculated according to equation (3).

$$\%\, of\ viable\ cells = Live\ cells\ /\ Total\ number\ of\ cells \quad (3)$$

Cell proliferation

CellTrace labelling. Cell labelling was performed with oMSC cells using CellTrace carboxyfluorescein succinimidyl ester (CFSE). For the labelling, cells were incubated with trypsin-EDTA for 5 min, centrifuged, and resuspended in 1 mL of PBS 1X (without Ca^{2+} and Mg^{2+}). Cells were incubated with 1 mL CellTrace CFSE (5–10 µM) in PBS 1X for 20 min at 37°C. Subsequently, to remove the unconjugated CellTrace, cell suspensions were incubated with DMEM supplemented with 5% (v/v) FBS for 5 min at 37°C. Cells were centrifuged, resuspended in DMEM supplemented with 10% (v/v) FBS and analysed as described below.

Cell labelling efficacy. To evaluate the efficacy of the labelling, CFSE + oMSCs were seeded at 20,000 cells/cm^2 in 24-well plates in DMEM supplemented with 10% (v/v) FBS and allowed to grow up to 7 days. On days 1, 3 and 7 cells were analysed by flow cytometry to quantify the remaining percentage of labelled cells. CFSE positive oMSCs were detected using the blue 488 nm laser channel (FL1). Non-stained cells were included as a control. Cells were analysed in FACSCalibur flow cytometer collecting at least 10,000 events. CellQuest software was used for data analysis.

Cell viability. The effect of the CellTrace on the metabolic activity of CFSE+oMSCs was evaluated by PrestoBlue Assay. Cells were seeded at 20,000 cells/cm^2 in a 24-well plate in DMEM/F12 supplemented with 10% (v/v) FBS and allowed to grow for up to 7 days. On days 1, 3 and 7 cells were analysed following manufacturer instructions. Non-stained cells were used as a control in each experiment.

Cell proliferation. CFSE+oMSCs were embedded into hydrogels of different stiffness and allowed to proliferate. On days 1, 3 and 7 samples were dissolved in 0.1 M EDTA and 0.5 M sodium citrate solution at 37°C for 10 min. Samples were then centrifuged at 300*g* for 5 min and resuspended in 500 µL of PBS. Cells were analysed by flow cytometry as described above.

Nutrients uptake

A glucose stock solution was prepared by dissolving 5 mg 2-NBGD in 1 mL of PBS. Glucose uptake was monitored by adding 68.85 µL of 2-NBDG stock solution to 5 mL of complete media obtaining a working solution of 0.06845 mg/mL. Briefly, 50,000 cells were embedded into hydrogels or seeded in 2D as control. After 24 h, 500 µL 2-NBGD working solution was added to the hydrogels and to the 2D control. After either 1 or 3 h incubation hydrogels were dissolved using 500 µL of dissolving buffer (0.1 M EDTA and 0.5 M sodium citrate, pH 7.4). Cells were washed twice with PBS to remove the excess of 2-NBGD and finally resuspended in 500 µL of PBS. Next, cells were analysed by flow cytometry to quantify the percentage of fluorescent cells. 2-NGBD positive oMSCs were detected using the blue 488 nm laser channel (FL1). Non-stained cells were included as a control. Cells were analysed in FACSCalibur flow cytometer collecting at least 10,000 events. CellQuest software was used for data analysis.

Cell morphology analysis

To qualitatively assess cell morphology of embedded cells, Phalloidin Dylight 550 was used. Hydrogels were fixed with 500 µL of 4% PFA for 1 h and permeabilised with 0.2% Triton X-100 in PBS for 20 min. Non-specific binding sites were blocked by incubating the cells in 2% bovine serum albumin in PBS for 1 h. Cells were stained with Phalloidin Dylight 550 (2 units/mL, stock solution 300 units/mL in methanol) for 2 h. Nuclei counterstaining was performed by incubating cells with DAPI (1:2000 dilution) for 15 min. Subsequently, hydrogels were washed twice with PBS. Lastly, hydrogels were imaged using confocal laser scanning microscope at 405 and 543 nm channels.

RNA extraction and RT-qPCR

Hydrogels were homogenised with a pellet pestle (Thomas Fisher Scientific, USA) in 0.7 mL qiazol and centrifuged at 18,000*g* for 2 min at room temperature. The supernatant was transferred into a fresh Qiashredder column (Qiagen, Switzerland) and centrifuged for 2 min at 18,000*g* at room temperature. Total RNA was extracted using the RNeasy Micro Kit according to manufacturer's instructions. RNA concentration and quality were measured using a NanoDrop (ND-1000; NanoDrop Technologies, Wilmington, DE, USA). Total RNA (250 ng from each sample) was reverse transcribed into cDNA using the High-Capacity cDNA

Reverse Transcription Kit on a thermal cycler (T100, Biorad, Watford, UK), according to manufacturer's instructions. qRT-PCR was performed in a QuantStudio™ 5 Real-Time PCR System (Applied Biosystems™, Fisher Scientific Loughborough, UK) using SsoAdvanced Universal SYBR Green Supermix and ovine specific primers reported in Supplemental Table 1.

Immunostaining

On day 21 hydrogels were fixed with 500 µL of 4% PFA for 1 h and rinsed three times with PBS. Hydrogels were then incubated overnight in a 30% w/v sucrose solution at 4°C. The next day the samples were placed in OCT and frozen in an isopentane bath previously chilled in liquid nitrogen and stored at −80°C for at least 1 day before sectioning. Sections of 20 µm were cut with a cryostat (Leica CM3050 S Cryostat, Leica Biosystems, Milton Keynes, UK) and mounted on SuperFrost™ Microscope Slides and left to dry for 30 min. Before staining the slides were fixed in ice cold acetone for 10 min at −20°C and left to dry for 30 min. Antigen retrieval was performed by using TRIS/EDTA buffer (10 mM Tris base, 1 mM EDTA solution, 0.05% Tween 20, pH 9.0) at 95°C for 10 min. Samples were rinsed once in PBS and incubated 30 min in a blocking buffer containing 2.5% w/v of BSA. Samples were then incubated with primary antibodies overnight at 4°C. The next day samples were rinsed 3 times with PBS and incubated with secondary antibodies for 1 h at room temperature. Nuclei counterstaining was performed by incubating cells with DAPI (1:2000 dilution) for 15 min. A full list of antibodies and dilutions is reported in Supplemental Table 2. Samples were then washed three times with PBS and mounted with aqueous fluorescent mounting media and imaged using a confocal laser scanning microscope LSM880 at 405, 488 and 594 nm.

Statistical analysis

Data are expressed as the mean ± standard deviation (SD). All experiments were conducted in triplicate. Experiments involving cells were conducted using cells from three different animal donors and each cell batch was further tested in triplicate. Comparison between groups was assessed by either ordinary one-way ANOVA or two-way ANOVA, followed by Tukey's multi-comparison test as indicated in the caption of each figure. The statistical analysis was performed with GraphPad Prism 8.0.2 (La Jolla, CA, USA), data were considered significant when $p < 0.05$.

Results

Hydrogels characterisation

Alginate/collagen (alg/col) hydrogels were crosslinked with increasing concentrations of $CaCl_2$ (30–100 mM) and their Young's modulus was measured by rheological assessment (Supplemental Figure 1 and Table 1).

Overall the increasing concentration of $CaCl_2$ led to the formation of hydrogels with increasing stiffness, with Young's modulus ranging from 0.82 to 6.85 kPa. The 3D structure of the hydrogels was analysed by image analysis from XCT tomograms (Figure 1). The col/alg hydrogels crosslinked with the lower concentration of $CaCl_2$ were characterised by a highly interconnected porous structure, with an overall porosity of 68.17% and an average pore diameter of 140.10 µm (Table 1). Conversely, the col/alg hydrogels crosslinked with 60 and 100 mM $CaCl_2$ appeared to have an inner porous core and an outer region characterised by small pores in the size range between 7.89 and 29.96 µm and an overall porosity of 27.29% and 42.65%, respectively. For the gel crosslinked with 60 mM $CaCl_2$ the average pore diameter was 22.15 µm, with over 58.77% of the pores in the range of 11.36–19.85 µm and these smaller pores were mainly present in the outer area of the hydrogels. The gels crosslinked with 100 mM $CaCl_2$ were characterised by an average pore diameter of 42.57 µm and over 47% of the pores were in the range of 11.36–19.85 µm.

SEM images of the col/alg hydrogels surface revealed that all hydrogels were characterised by a smooth non-porous surface with visible collagen fibres (Figure 2(a) and (b)). SEM images were also taken after 7 and 14 days of incubation of the hydrogels in PBS to assess their degradation; loss of integrity and formation of a highly porous surface were evident (Figure 2(c) and (d)). The col/alg hydrogels crosslinked with the 30 mM $CaCl_2$ lost 70% weight after 7 days and over 90% after 14 days (Figure 2(e)). The other two formulations were characterised by a slower degradation rate with a weight loss of 40% for the 60 mM and 50% for the 100 mM formulation at day 7 and an overall weight loss of 81% at day 14 for both (Figure 2(e)).

oMSC characterisation

Immunophenotypic characterisation of oMSCs was performed at passage 2, all samples showed positivity to CD44 and CD29 (mesenchymal marker) and were negative for CD45 and CD34 (haematopoietic stem cell markers), indicating that the cells were not of haematopoietic origin (Figure 3(a)). oMSCs were successfully differentiated into osteoblasts, chondrocytes and adipocytes in 21 days (Figure 3(b)).

Hydrogels cytocompatibility

oMSCs were encapsulated into col/alg hydrogels of different stiffness and the viability was evaluated at day 1 and 7 (Supplemental Figure 2). A quantitative analysis of cell viability (Figure 4(a)) revealed that 90% of cells were viable within the hydrogels with no significant difference among the formulations.

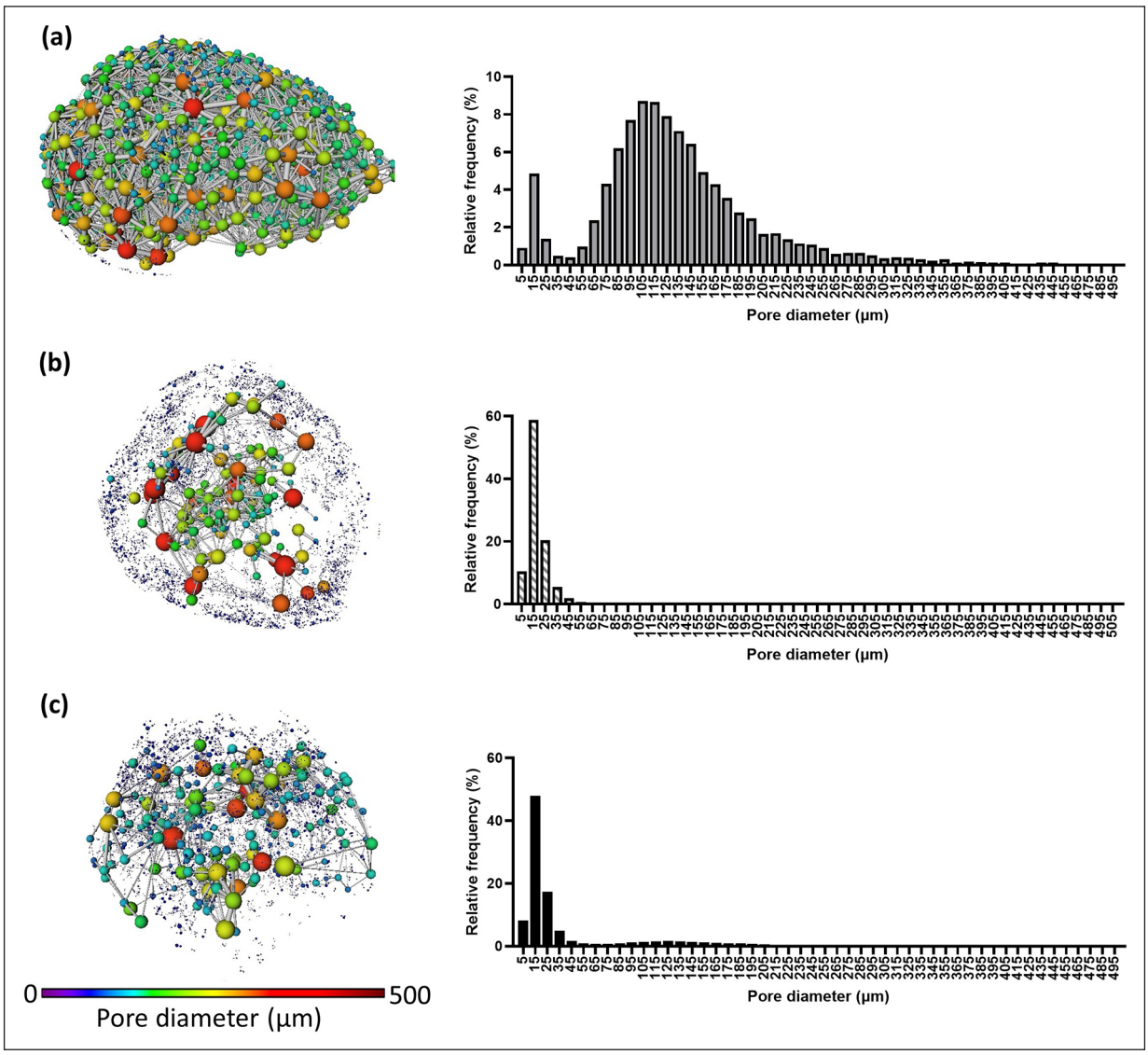

Figure 1. Representative 3D pore network from the XCT reconstruction of hydrogels crosslinked with (a) 30 mM $CaCl_2$ – corresponding to 0.82 kPa stiffness, (b) 60 mM $CaCl_2$ – corresponding to 5.75 kPa stiffness and (c) 100 mM $CaCl_2$ – corresponding to 6.85 kPa stiffness, their 3D pore network and pore distribution ($n = 3$). Both D'Agostino and Pearson's and Kolmogorov-Smirnov's normality test returned $p < 0.001$ for all gels.

To further evaluate the cytocompatibility of the hydrogels, nutrient uptake was assessed using a fluorescent glucose probe (2-NBGD), this was added to the media and the percentage of positive cells was determined through flow cytometry after 1 and 3 h (Supplemental Figure 3). After 1 h, more than 50% of cells resulted positive for glucose in all formulations, with over 70% of cells positive for glucose in the softer hydrogel (Figure 4(b)). After 3 h in all three formulations, the percentage of positive cells was over 75% without any significant difference between the 5.75 and 6.85 kPa hydrogels. Cell proliferation was assessed using CFSE Celltrace staining, where a reduction of fluorescence overtime indicates the proliferation of oMSCs.[52,53] To establish cell proliferation within the hydrogel the first step was to validate cell labelling using Cell Trace dye (Supplemental Figure 4). Since CellTrace binds covalently to all free amines on the surface and inside of cells, through subsequent cell divisions, daughter cells receive approximately half of the fluorescent label of their parent cells, allowing the analysis of the fluorescence intensities of labelled cells. Data showed a reduction of fluorescence overtime indicating that oMSC embedded into the hydrogels are proliferating (Figure 5(a)). On day 1 no significant difference was found for oMSC embedded into hydrogels of different stiffness. On day 7 cells embedded into the 0.82 kPa hydrogels were characterised by a significantly higher proliferation rate compared to the cells encapsulated in the 5.75 and 6.85 kPa hydrogels (Figure 5(b)).

Table 1. Rheological parameters and porosity data for col/alg hydrogels crosslinked with different $CaCl_2$ concentrations. Data are reported as mean ± SD ($n = 3$).

$CaCl_2$ concentration	30 mM	60 mM	100 mM	One-way ANOVA	Tukey's post-hoc multicomparison test
Loss modulus (kPa)	0.27 ± 0.06	1.87 ± 0.46	2.56 ± 0.38	$p < 0.01$	30 vs 60 mM $p < 0.0001$ 30 vs 100 mM $p < 0.0001$ 60 vs 100 mM $p < 0.0001$
Storage modulus (kPa)	0.04 ± 0.02	0.42 ± 0.06	0.61 ± 0.07	$p < 0.001$	30 vs 60 mM $p < 0.0001$ 30 vs 100 mM $p < 0.0001$ 60 vs 100 mM $p < 0.05$
Complex modulus (kPa)	0.27 ± 0.06	1.91 ± 0.40	2.28 ± 0.49	$p < 0.0001$	30 vs 60 mM $p < 0.0001$ 30 vs 100 mM $p < 0.0001$ 60 vs 100 mM $p < 0.05$
Young's modulus (kPa)	0.82 ± 0.19	5.75 ± 1.15	6.85 ± 1.12	$p < 0.0001$	30 vs 60 mM $p < 0.0001$ 30 vs 100 mM $p < 0.0001$ 60 vs 100 mM $p < 0.05$
Porosity (%)	68.17 ± 5.93	27.29 ± 2.46	42.65 ± 13.51	$p < 0.001$	30 vs 60 mM $p < 0.01$ 30 vs 100 mM $p < 0.05$ 60 vs 100 mM $p > 0.05$
Average pore diameter (μm)	140.1 ± 6.54	22.15 ± 2.02	42.57 ± 25.80	$p < 0.0001$	30 vs 60 mM $p < 0.01$ 30 vs 100 mM $p < 0.01$ 60 vs 100 mM $p > 0.05$

oMSC morphology in hydrogels of different stiffness

oMSC grown in 2D culture are characterised by a spindle shape morphology, when embedded into the soft hydrogels oMSCs acquired a rounded chondrocyte-like morphology and on day 7 started to form small aggregates of cells. In particular, the formation of aggregates was more evident in the 0.82 and the 5.75 kPa hydrogels, with the latter presenting better defined and larger aggregates (Figure 6).

Gene expression analysis

To monitor how stiffness affects the ability of oMSC to differentiate into chondrocytes, gene expression analysis was performed at days 1, 7 and 14 (Figures 7 and 8). The analysis compared the level of *SOX9*, the master regulator of chondrogenesis, and *RUNX2*, a transcription factor involved in the osteogenic differentiation of MSCs. On day 1 a significant increase in the expression of *SOX9* was observed in all formulations, with over 500-fold increase compared to the 2D control. A high level of *SOX9* expression was maintained to day 7 in the 5.75 kPa hydrogel, while it significantly decreased on the 0.82 and 6.85 kPa hydrogels. Interestingly an increase of *RUNX2* was observed at day 1 in all formulations, with a stable expression over 14 days in the 6.85 kPa substrate. oMSC embedded into the 5.75 kPa hydrogels showed an increase in the expression of *RUNX2* both at day 1 and 7, which drastically decreased at day 14. Even though a significant increase of *RUNX2* was observed in all formulations compared to the 2D control, the ratio analysis between *SOX9* and *RUNX2* revealed that on day 1 the expression had significantly shifted towards the chondrogenic lineage and remained higher at day 7 and 14 in the 5.75 kPa compared to the other two formulations.

In order to investigate the differences in gene expression for extracellular matrix components associated with the formation of cartilage in different gels *COL2A1*, *ACAN* and *COL1A1* were evaluated (Figure 8). The expression of *COL2A1* significantly increased at day 1 within all formulations, with a more significant effect in the 5.75 kPa hydrogel where the expression was 2000-fold higher than the 2D control and twice the expression of *COL2A1* in the 0.82 and 6.86 kPa hydrogels. Furthermore, the expression of *COL2A1* in the 5.75 kPa substrate at day 7 remained 58-fold and 10-fold higher than on the 0.82 and 6.75 kPA substrates, respectively. In particular, a significant decrease in the expression of *COL2A1* was observed in the softer hydrogels at day 7. Stiffness affected the expression of *ACAN* as well (Figure 8). A positive effect of the 5.75 kPa stiffness was observed in the expression of *ACAN* both on day 1 and 7. The 0.82 kPa hydrogel was characterised by a significant increase in the expression of *ACAN* at day 1 followed by a significant decrease at day 7 and 14. As the experiments were conducted in the absence of growth factors the expression of *COL1A1* was measured to investigate the effect of stiffness on the expression of hypertrophic markers. Interestingly, a significant downregulation of *COL1A1* on day 1 in all the substrates was observed compared to the 2D control. On day 7 an increase in the expression of *COL1A1* was observed in the 0.82 and 5.75 kPa

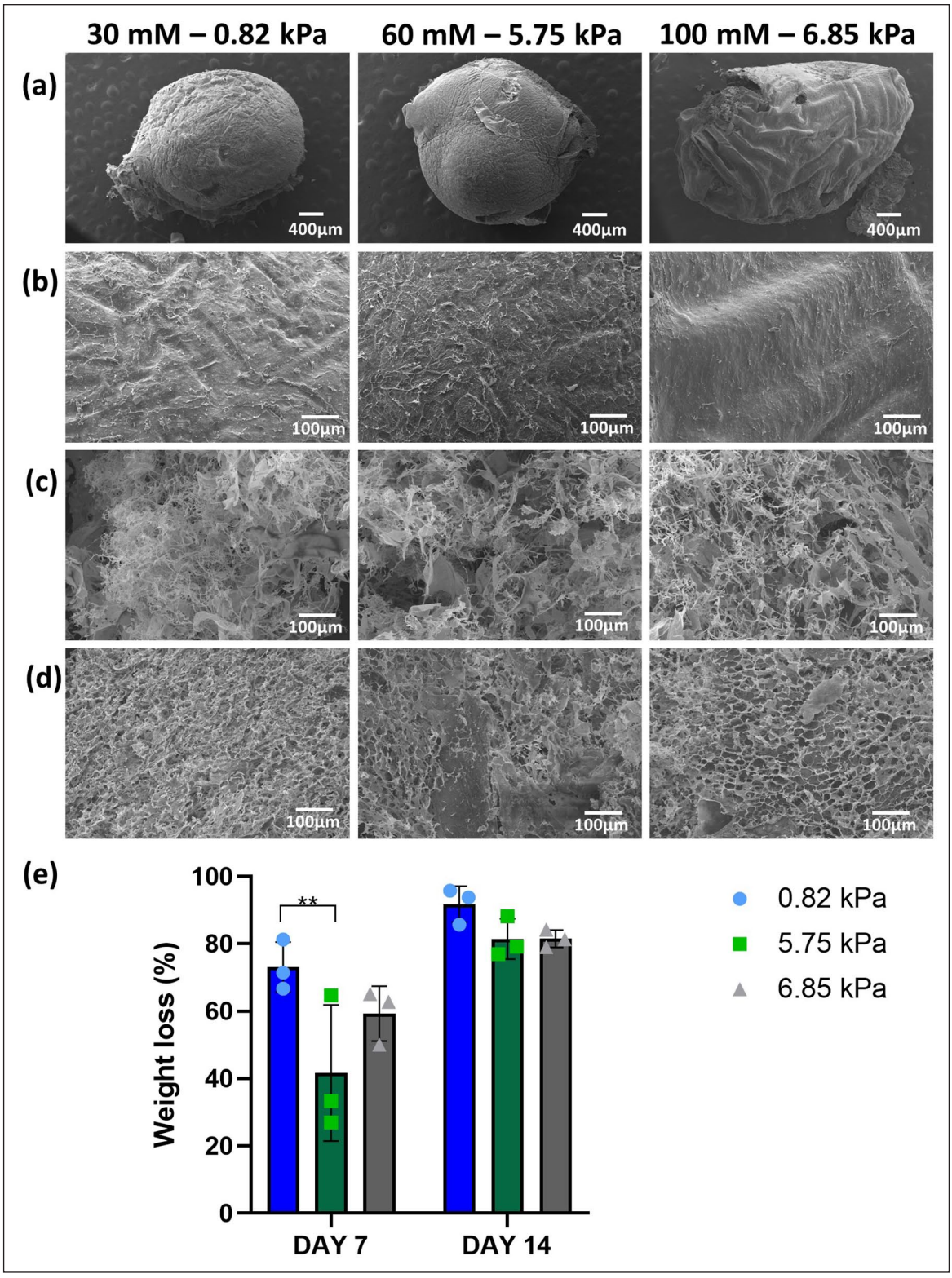

Figure 2. Degradation of col/alg hydrogels crosslinked with 30, 60 and 100 mM $CaCl_2$ incubated in PBS at 37°C. (a) SEM images of the surface of col/alg hydrogels and (b) at higher magnification before the degradation studies. SEM images of the surface of col/alg hydrogels on (c) day 7 and (d) 14 of degradation. (e) Weight loss of hydrogels during the degradation study. Data re reported as mean ± SD ($n = 6$). Comparison between groups was assessed by ordinary two-way ANOVA (time effect $p < 0.001$, stiffness effect $p > 0.05$) using post hoc Tukey's test (** $p < 0.001$).

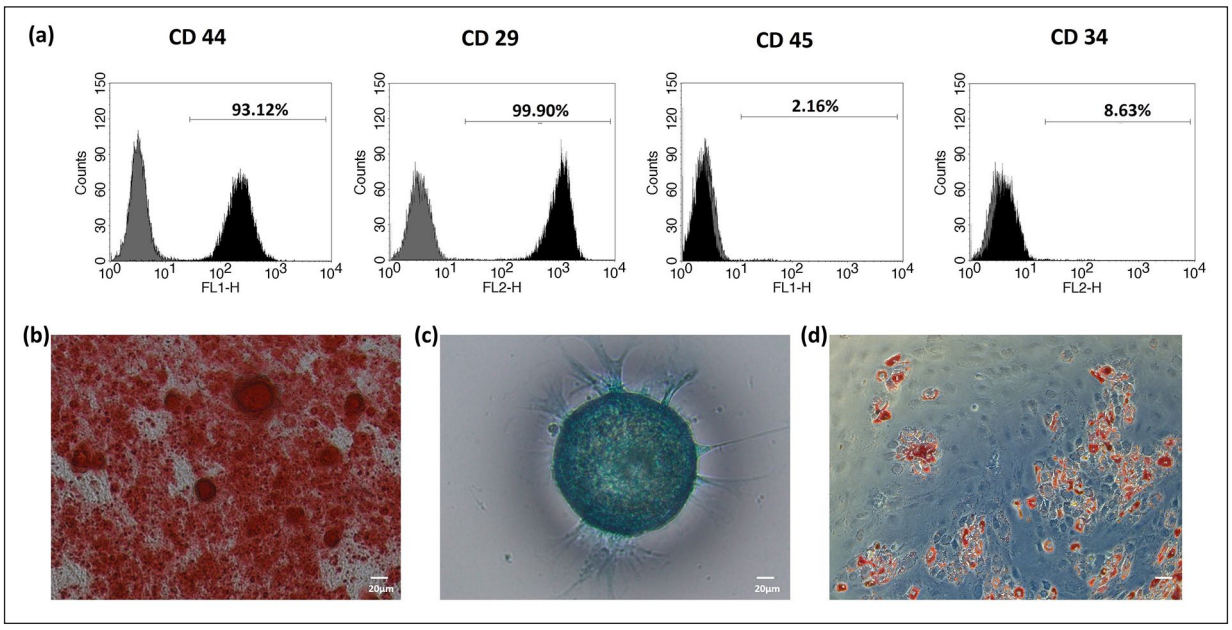

Figure 3. Surface marker expression analysis of ovine MSCs and osteogenic, chondrogenic and adipogenic differentiation. (a) Phenotypic characterisation by flow cytometry of a representative population of oMSCs. The black histogram represents the specific antibody, while the grey histogram represents the isotype control. Markers characteristic of MSCs (CD29, CD44) and haematopoietic cells (CD45, CD 34). (b) Alizarin red S (osteogenesis), (c) Alcian Blue (chondrogenesis) and (d) Oil Red O (adipogenic) staining of differentiated stem cells at day 21.

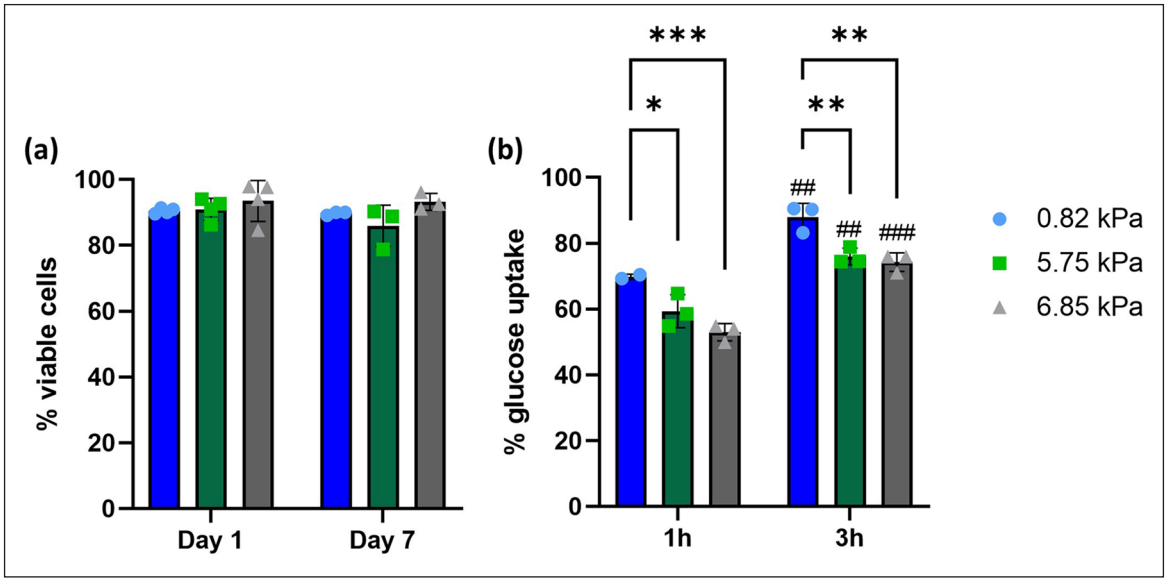

Figure 4. Viability of oMSC and nutrients diffusion in hydrogels of different stiffness. (a) Quantitative analysis of the cell viability. Data are reported as mean ± SD ($n = 3$). Comparison between groups was assessed by ordinary two-way ANOVA (time and stiffness effect $p > 0.05$) followed by a post-hoc Sidak's test. (b) Quantitative analysis of 2-NBDG uptake by oMSC embedded into hydrogels of different stiffness after 1 and 3 h. Data are reported as mean ± SD ($n = 3$). Comparison between groups was assessed by ordinary two-way ANOVA (time effect $p < 0.0001$ and stiffness effect $p < 0.01$) using post hoc Sidak's test ($^{*}p < 0.01$, $^{**}p < 0.001$ and $^{\#\#}p < 0.01$, $^{\#\#\#}p < 0.001$ comparing time points).

hydrogels. However, in both formulations, the expression of *COL1A1* significantly decreased at day 14 (Figure 8). Furthermore, the gene expression analysis revealed that at day 14 the expression of *COL1A1* was significantly lower compared to the 2D control. *COL2A1* and *COL1A1* expression were compared and the ratio between the two genes revealed that over time the expression of *COL2A1* was higher in all formulations.

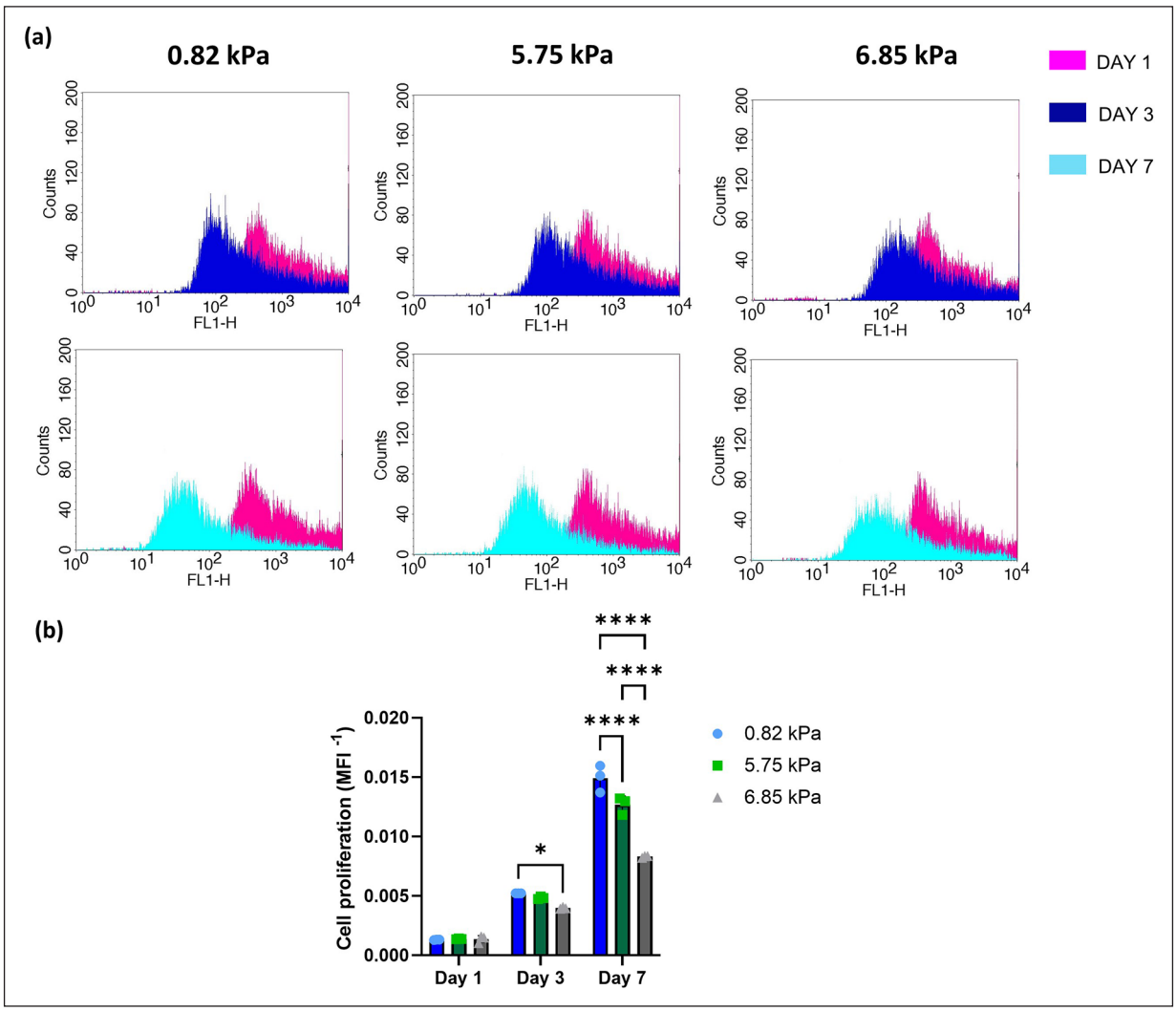

Figure 5. (a) Flow cytometry histogram of the frequency distribution of CFSE stained oMSC at day 1, 3 and 7. (b) Proliferation of oMSCs into hydrogels of different stiffness at day 1, 3 and 7. Data are reported as mean ± SD ($n = 3$). Comparison between groups was assessed by ordinary two-way ANOVA (time and stiffness effect $p < 0.0001$) followed by a post-hoc Tukey's test (*$p < 0.01$, ****$p < 0.0001$).

Immunostaining of ECM proteins

To investigate the effect of stiffness on ECM deposition, immunofluorescence analysis was conducted at day 21 to determine the composition of the extracellular matrix. Collagen type II and aggrecan staining was performed to assess the synthesis of ECM typical for cartilage (Figure 9). Deposition of ECM was observed in all formulations. Due to its higher degree of porosity and degradation rate, the softest substrate did not support the formation of intact tissue (Figure 9(a)). Furthermore, the deposition of the cartilaginous matrix was significantly lower compared to the 5.85 and 6.85 kPa substrates as shown by the mean intensity fluorescence (MIF) analysis (Figure 9(d)). Higher deposition of collagen type II and aggrecan was evident in the 5.75 kPa substrate and was further confirmed by the MIF analysis (Figure 9(b), (d) and (e)). Even though all three soft substrates direct stem cell fate into a cartilage phenotype, affecting both gene expression and ECM deposition, they did not prevent hypertrophy as shown by the deposition of collagen type I. In fact, the immunofluorescence analysis revealed that collagen type I, a marker of cartilage hypertrophy, was present in all formulations, showing significantly higher deposition in the 0.82 and 6.85 kPa substrates compared with the 5.75 kPa hydrogel. The MIF analysis revealed that oMSC embedded into the 5.75 kPa hydrogels deposited a significantly lower amount of collagen type I.

Discussion

A successful strategy to differentiate MSCs into a stable chondrocytic population that does not have a propensity to undergo hypertrophy when implanted in vivo is still

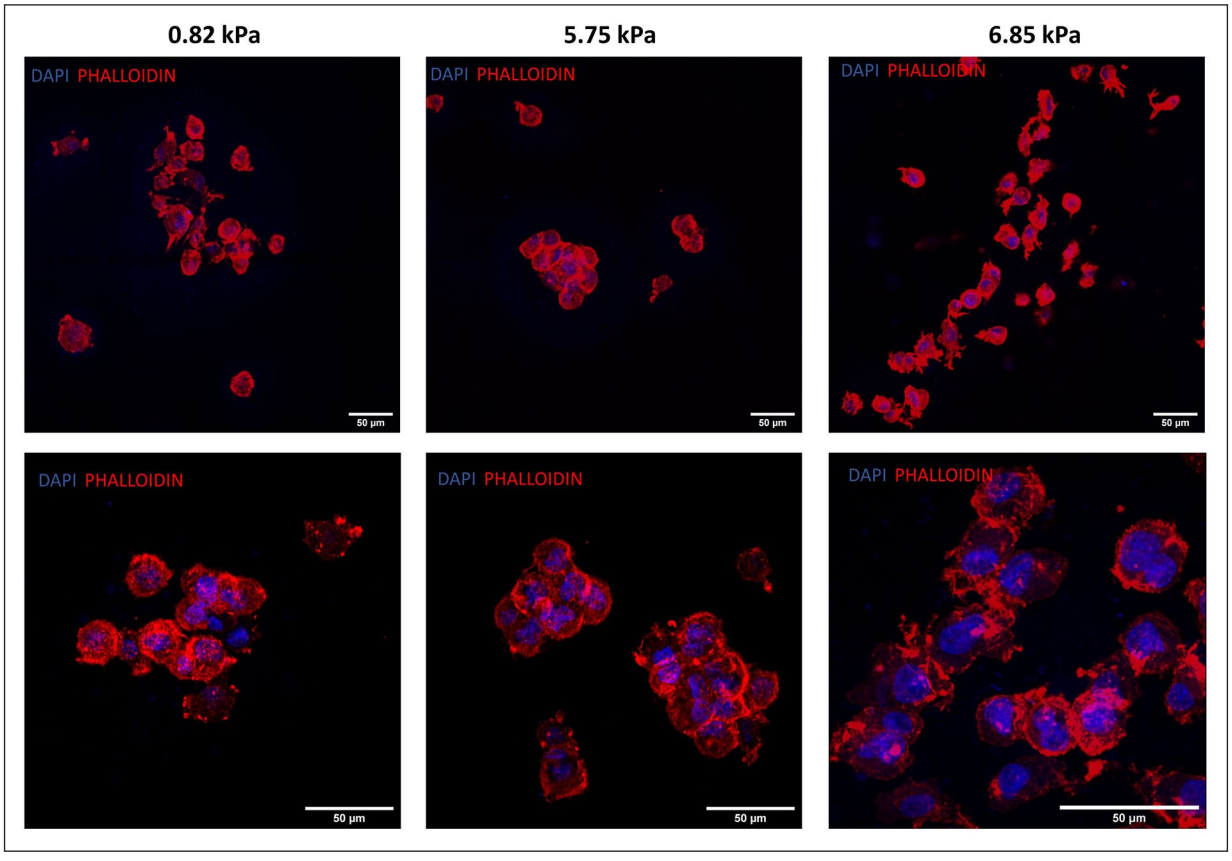

Figure 6. Morphological characterisation of oMSCs at day 7 embedded into hydrogels of different stiffness. Representative confocal images of oMSCs at day 7 stained with phalloidin and DAPI.

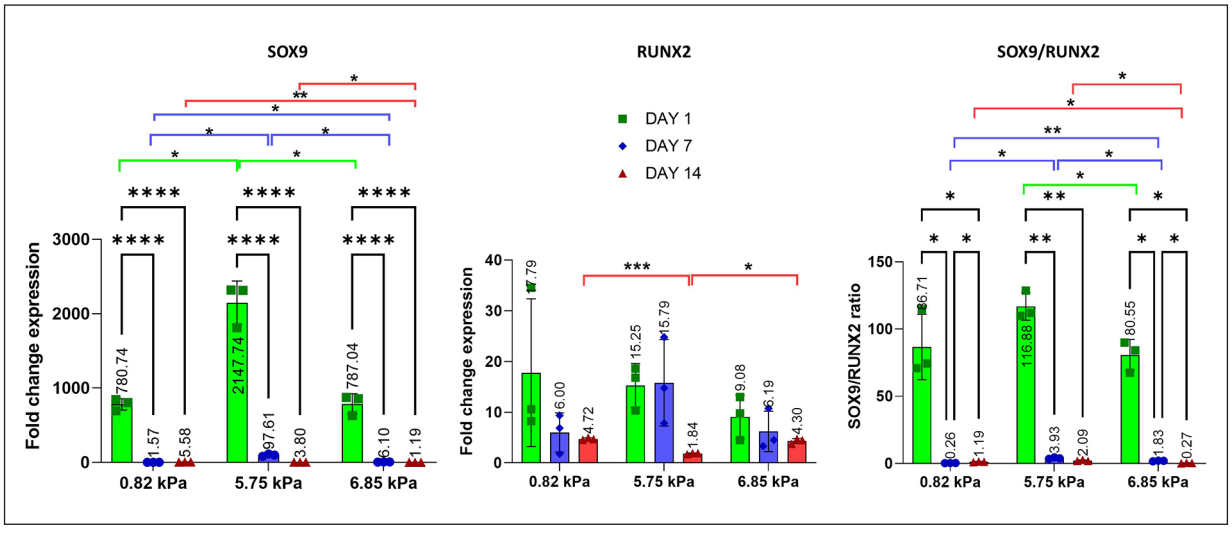

Figure 7. Gene expression of *SOX9*, *RUNX2* and *SOX9/RUNX2* of oMSC embedded into col/alg hydrogels of different stiffness at day 1, 7 and 14. mRNA data are presented as fold change relative to 2D control. Results represent mean ± SD ($n = 3$). Comparison between groups was assessed by ordinary two-way ANOVA effect of time $p < 0.0001$ for *SOX9*, $p < 0.05$ for *RUNX2*, $p < 0.0001$ for *SOX9/RUNX2*; effect of stiffness $p < 0.0001$ for *SOX9*, $p > 0.05$ for *RUNX2*, $p > 0.05$ for *SOX9/RUNX2*) followed by a post hoc Tukey's test (* $p < 0.01$, ** $p < 0.001$, **** $p < 0.0001$).

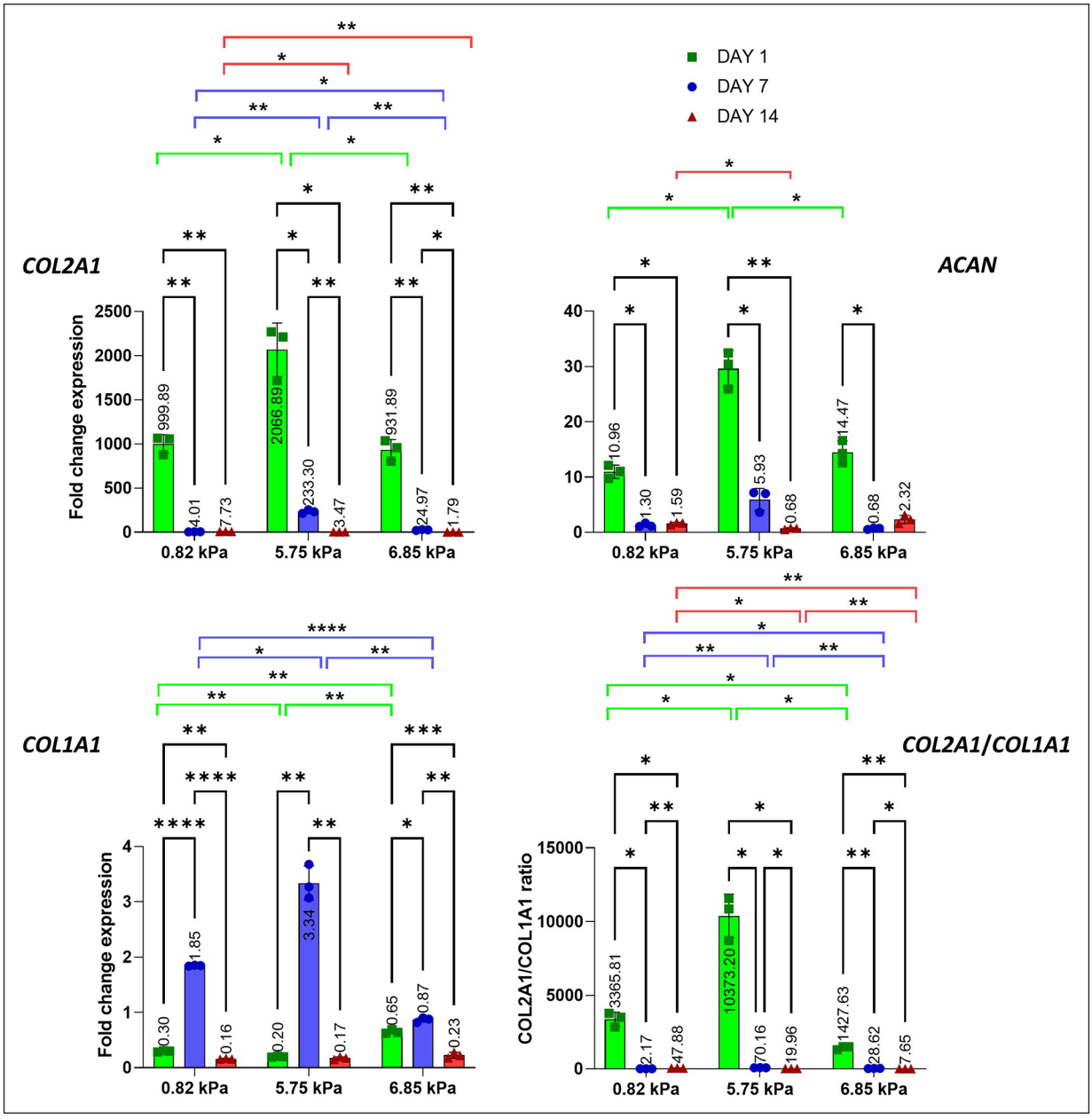

Figure 8. Gene expression of ECM protein *COL2A1*, *ACAN*, *COL1A1* and *COL2A1/COL1A1* of oMSC embedded into col/alg hydrogels of different stiffness at day 1, 7 and 14. mRNA data are presented as fold change relative to 2D control. Results are reported as mean ± SD ($n = 3$). Comparison between groups was assessed by ordinary two-way ANOVA (effect of time $p < 0.0001$ for *COL2A1*, *ACAN*, *COL1A1* and *COL2A1/COL1A1*; effect of stiffness $p < 0.001$ for *COL2A1* and $p < 0.0001$ for *ACAN*, *COL1A1* and *COL2A1/COL1A1*) followed by a post hoc Tukey's test (*$p < 0.01$, **$p < 0.001$, ****$p < 0.0001$).

lacking. Today most studies use growth factors to guide the differentiation of MSCs into chondrocytes.[54–59] The widespread use of TGF-β to guide chondrogenic differentiation has been shown to lead to the overexpression of hypertrophic markers even after only 1 day of exposure.[16] This will eventually lead to the formation of fibrocartilage, characterised by the production of collagen type I and inferior mechanical properties compared to hyaline cartilage. The present study aimed at developing hydrogel formulations of low stiffness to recapitulate the conditions found in the soft environment of the limb bud, and use them to evaluate the effect of substrate stiffness in directing MSCs differentiation towards the chondrogenic lineage without the use of growth factor. Soft col/alg hydrogels were successfully produced, and their stiffness was tuned by employing different concentrations of crosslinker, offering a simple model for encapsulating MSCs and studying their behaviour. The rheological analysis revealed that Young's modulus was within the range of 0.82–6.85 kPa, which has previously been shown to be favourable for the

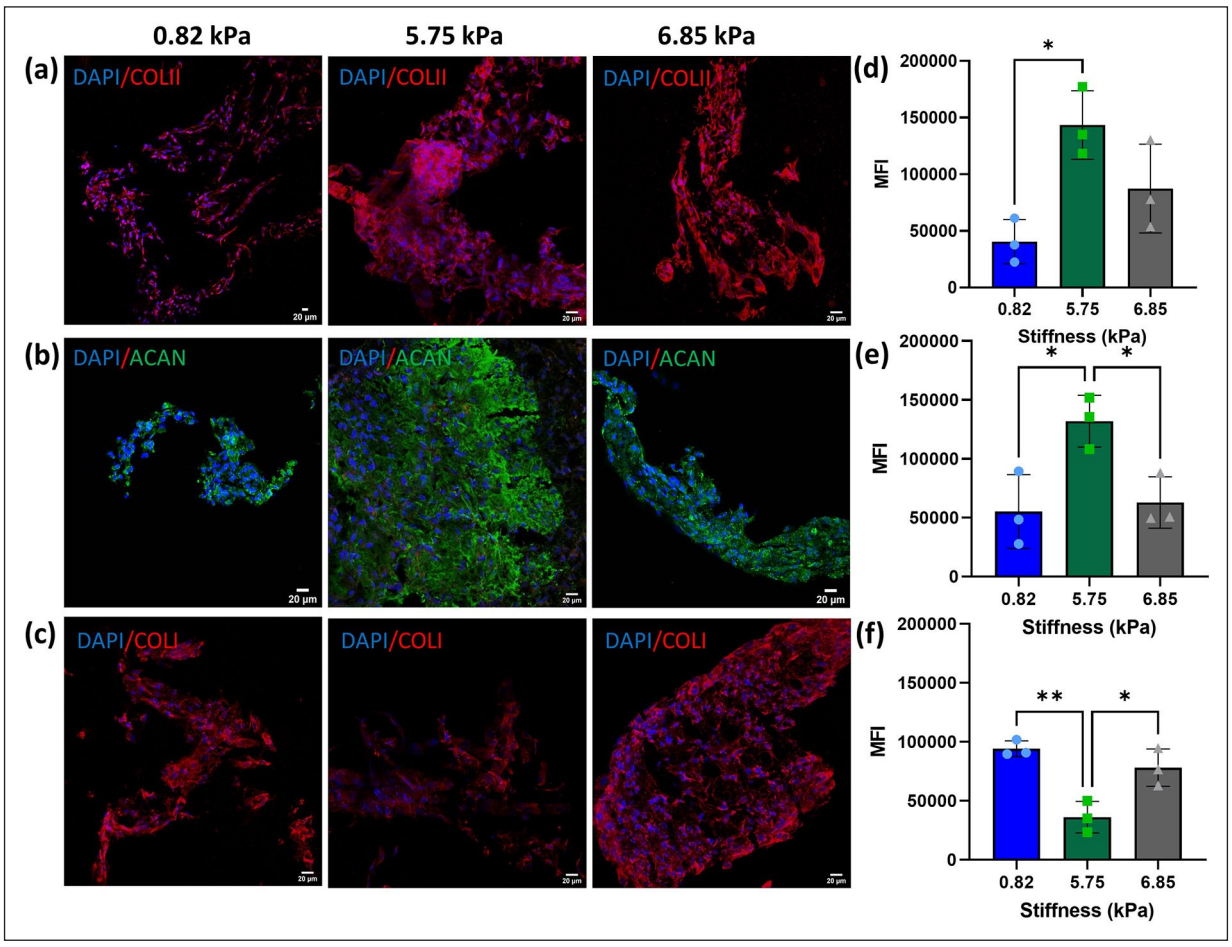

Figure 9. Immunofluorescence images of ECM deposition at day 21 and quantitative analysis of the mean intensity fluorescence. Representative confocal images of (a) collagen type II, (b) aggrecan and (c) collagen type I staining at day 21 in hydrogels of different stiffness. Quantitative analysis of mean fluorescence intensity (MFI) of (d) collagen type II, (e) aggrecan and (f) collagen type I in hydrogels of different stiffness at day 21. Data are reported as mean ± SD, $n = 3$. Comparison between groups was assessed by ordinary one-way ANOVA ($p < 0.05$ for COLI and ACAN, $p < 0.01$ for COLII) followed by a post-hoc Tukey's test (*$p < 0.05$, ** $p < 0.01$).

differentiation of MSCs into chondrocytes.[21,33,37] Even though soft substrates do not mimic the stiffness of native cartilage, they appear to simulate the mechanical properties of the developing limb bud, suggesting that developing soft substrates simulating the mechanical properties of cartilage development could represent a promising strategy for directing MSCs into chondrocytes.[21,38] SEM images of intact hydrogels showed the presence of an outer membrane for each hydrogel. However, XCT analysis revealed that the 0.82 kPa hydrogels were characterised by a higher porosity, compared to the 5.75 and 6.85 kPa that were characterised by a ticker outer membrane of smaller pores, and an inner highly interconnected porous core. However, it is unlikely that the hydrogels are able to maintain the size of these pores when hydrated, nevertheless characterisation of the porosity of dry gels is important as it provides information on the most appropriate gel for cell encapsulation, differentiation, proliferation, migration and extracellular matrix production. The presence of an outer membrane might be due to the use of $CaCl_2$ as crosslinking agent. Due to its high solubility in water the gelation rate of alginate is too high to control, and leads to the formation of an outer membrane as soon as the drop of col/alg mixture enters the $CaCl_2$ bath.[44] Gelation rate affects gel uniformity and strength, in fact though the col/alg hydrogel crosslinked with 100 mM of $CaCl_2$ were characterised by higher Young's modulus, both the XCT and rheological analysis showed a non-uniform and weaker structure characterised by reversible crosslinking at higher frequencies, which was not observed in the other two formulations. In order to control the porosity and the thickness of the outer shell, crosslinking time could be adjusted and different exposure times to $CaCl_2$ could be tested.[43] The presence of a thicker shell allowed for better cell encapsulation within the gels without affecting nutrient diffusion into the hydrogel or hampering the migration and proliferation of the

encapsulated cells. Degradation studies performed without cells revealed that all three hydrogels lost over 90% of their weight over 14 days. Conversely, when oMSCs were embedded into the 5.75 and 6.85 kPa hydrogels they remained intact for 21 days, suggesting that ECM deposition affected the integrity of the hydrogels. The integrity of the gel with cells at 21 days may be explained by greater cell proliferation, cell aggregation and matrix deposition. When embedded into the 0.82 kPa hydrogel, for which the weight loss at day 7 was 70%, oMSC did not form an intact tissue and at day 21, the immunofluorescent analysis revealed that oMSCs in this gel were characterised by lower matrix deposition and smaller cell aggregates with large gaps between the cells suggesting that the degradation rate of the hydrogels was higher than the ECM deposition. The stiffness of the gel did not affect cell viability over time, however, it affected oMSCs proliferation which at day 7 was significantly higher in the 0.82 and the 5.75 kPa substrates compared to the 6.75 kPa hydrogel. It is well known that stiffness regulates cell proliferation, however, previous studies have shown that stiffer substrates increase cell proliferation compared to soft substrates. We hypothesised that the increased proliferation rate on 0.82 and 5.75 kPa hydrogels might be associated with cells aggregation which is known to improve cell viability and proliferation.[60] The effect of stiffness in directing MSCs behaviour was first demonstrated by Engler et al.[25] Their work suggested that, when pre-conditioned on a specific stiffness, MSCs couldn't be reprogrammed even with the use of growth factors. Park et al. highlighted the importance of stiffness, in particular of soft substrates (1 kPa), in directing MSCs towards the chondrogenic and adipogenic lineage; however, they warned this effect may not be specific for only one lineage, and biochemical factors such as TGF-β are required.[61] In contrast, our work provided for the first-time evidence that soft substrates can direct oMSC towards the chondrogenic lineage without the use of any growth factor. MSCs sense the surrounding environment and respond to physical cues by changing their phenotype. Cytoskeleton reorganisation is known to be a key regulator of MSCs differentiation, as a spreading morphology has been demonstrated to promote osteogenesis.[62] On the other hand reduction in cells spreading and transition to rounded morphology is associated to chondrogenic differentiation.[63] Soft col/alg hydrogels provided a suitable 3D environment that reduced cells spreading and lead oMSCs to acquire a rounded morphology without stress fibres, this environment also aided cells migration and allowed the formation of aggregates. Furthermore, this work revealed that stiffness significantly affects the expression of the master regulator of chondrogenesis, *SOX9*, as well as *COL2A1* and *ACAN* already from day 1. Mesenchymal condensation represents the major event affecting MSCs commitment to the chondrogenic lineage and the stabilisation of *SOX9* and its expression is required during embryonic development as well as in post-natal maintenance of articular cartilage.[17] Here we showed that oMSC embedded into soft hydrogels started to condensate and formed small aggregates on day 7. However, our data reveal that stiffness might play a fundamental role in regulating MSCs fate even before mesenchymal condensation. In fact, gene expression analysis shows that soft substrates appear to affect the expression of *SOX9* from day 1 demonstrating that mechanical cues may be a way to successfully engineer functional cartilaginous tissues.

One of the main challenges in cartilage repair is the formation of fibrocartilage. Our work showed that the expression of *COL1A1*, a marker of hypertrophy, significantly decreased at day 14 compared to the 2D control. Furthermore, our data indicate that the 5.75 kPa hydrogel, did not only support ECM deposition but also limited the expression of *RUNX2* and the formation of fibrocartilage compared to the other hydrogels suggesting that even small changes in stiffness could have a significant effect on the hypertrophic phenotype of MSCs. These data are in accordance with Wang et al. that demonstrated that low mechanical stiffness (~1 kPa) led to the significantly higher deposition of type I collagen.[35] Although the role of stiffness has shown to play a crucial role in stem cells differentiation, the biological mechanism behind is still poorly understood. Stiff substrates appear to promote nuclear localisation of Yes associated protein (YAP) and Transcriptional coactivator with PDZ-binding motif (TAZ) which modulate RUNX2 transcriptional activation thus facilitating osteogenic differentiation, suggesting that scaffolds with stiffness matching the one of the articular cartilage might not be appropriate for chondrogenic differentiation of MSCs.[64–67] While on soft substrates MSC have shown increased nuclear localisation of SMAD 2/3 (involved in the initiation of chondrogenic differentiation), while SMAD 2/3 remained confined to the cytosol in MSCs on stiff substrates.[38,43] Further research should focus on understanding the biological mechanisms behind the regulation of chondrogenesis on soft substrates.

Another important result from this study is the efficacy in differentiating MSCs using a relatively low number of cells. In fact, usually chondrogenic differentiation of MSCs requires a high seeding density and pellet culture to allow a proper ECM formation.[68,69] This is one of the main limitations in the translation of MSC therapies. Lee and Wang have estimated that the dosage of MSC required for clinical efficacy is in the range of 40–100 million cells per knee.[11] However, soft col/alg hydrogels are able to differentiate oMSCs into chondrocytes using much smaller numbers of cells (1 million cells/mL) suggesting that the overall number of cells for clinical application could be reduced.

Although this work shows the importance of soft substrates in directing MSCs fate, in order to obtain chondrocytes able to produce large amounts of extracellular matrix

similar to articular cartilage, the introduction of other environmental cues might be important. The delayed exposure to hydrostatic pressure in combination with soft substrates might further enhance the formation of cartilaginous matrix and the increased expression of chondrogenic markers over time.[24,43,70,71] The addition of a mechanical stimulation such as hydrostatic pressure may regulate proliferation of cells and the deposition of extracellular matrix which may be important as the soft hydrogels will not be able to withstand the load articular cartilage is subjected to. Acclimatisation using mechanical stimulation of the cells and production of ECM within scaffolds before implantation, will increase the overall Young's modulus of the scaffold.[2] Hypoxia pre-conditioning should also be considered as an additional cue to enhance cartilage formation.[72–75] In vivo the oxygen tension within the cartilage varies between 2% and 5%, whilst the atmospheric oxygen level (20%) at which most typical tissue culture incubators operate is actually non-physiological and represents hyperoxia. MSCs cultured under hypoxic conditions have shown an increase in matrix formation along with a downregulation of hypertrophic markers.[72] Additionally, hypoxia preconditioning could not only enhance cartilage formation in vivo, but also support survival of MSCs when implanted into the tissue.[76,77]

One of the main limitations of this study from a translational perspective is the use of ovine mesenchymal stem cells. The choice of using oMSCs was taken because work would ultimately lead to implantation of the hydrogels within an animal model. Large animal models are commonly used for in vivo testing of biomaterials for cartilage repair due to the size of defects that can be created and the loads sustained by the cartilage which is closer to human levels than in a small animal models.[78–81] Although oMSC showed morphological, phenotypical and functional properties similar to those observed in their human counterparts, Haddouti et al. performed a comparative study between human and ovine MSC and demonstrated that oMSCs have a significantly higher capacity for chondrogenic differentiation compared to hMSCs.[82–84] Future research should focus on confirming the present results on human MSCs. In conclusion, this study demonstrated for the first time that soft col/alg hydrogels were able to direct mesenchymal stem cells differentiation into chondrocytes without the use of growth factors and allowed the deposition of cartilaginous matrix with limited formation of collagen type I. Furthermore, soft col/alg hydrogels allowed to obtain chondrogenesis even using a limited number of MSCs, suggesting that the stiffness of the substrate is a crucial mechanical cue in initiating and maintaining the chondrogenic differentiation of MSC and this could potentially reduce the overall number of cells required for clinical application. These gels were able to maintain a chondrocytic phenotype reducing the expression of hypertrophic genes. Soft hydrogels might be ideal to direct MSC chondrogenesis and mechanical properties should be carefully considered when developing a scaffold for cartilage repair.

Authors contributions

T.R. designed and carried out all experimental procedures, analysed the data and drafted the manuscript. R.B. carried out the computed tomography experiments and supervised the relative data analysis. G.B. supervised the project, critically reviewed the manuscript and acquired the funding. M.R. supervised the project, contributed to data analysis and drafting of the manuscript, critically reviewed the manuscript and acquired the funding.

Declaration of conflicting interests

The author(s) declared no potential conflicts of interest with respect to the research, authorship, and/or publication of this article.

Funding

The author(s) received no financial support for the research, authorship, and/or publication of this article.

ORCID iDs

Tosca Roncada https://orcid.org/0000-0002-8114-0595
Roxane Bonithon https://orcid.org/0000-0002-4252-0894
Marta Roldo https://orcid.org/0000-0003-2242-7761

Supplemental material

Supplemental material for this article is available online.

Data availability statement

The datasets generated and analysed during the current study are available from the corresponding author on reasonable request.

References

1. Nooeaid P, Salih V, Beier JP, et al. Osteochondral tissue engineering: scaffolds, stem cells and applications. *J Cell Mol Med* 2012; 16: 2247–2270.
2. Davis S, Roldo M, Blunn G, et al. Influence of the mechanical environment on the regeneration of osteochondral defects. *Front Bioeng Biotechnol* 2021; 9: 603408.
3. Lo Monaco M, Merckx G, Ratajczak J, et al. Stem cells for cartilage repair: preclinical studies and insights in translational animal models and outcome measures. *Stem Cells Int* 2018; 2018: 9079538.
4. Tamaddon M, Wang L, Liu Z, et al. Osteochondral tissue repair in osteoarthritic joints: clinical challenges and opportunities in tissue engineering. *Bio-Design Manuf* 2018; 1: 101–114.
5. Calabrese G, Forte S, Gulino R, et al. Combination of collagen-based scaffold and bioactive factors induces adipose-derived mesenchymal stem cells chondrogenic differentiation in vitro. *Front Physiol* 2017; 8: 50.
6. Mobasheri A, Kalamegam G, Musumeci G, et al. Chondrocyte and mesenchymal stem cell-based therapies for cartilage repair in osteoarthritis and related orthopaedic conditions. *Maturitas* 2014; 78: 188–198.

7. Liu Y, Shah KM and Luo J. Strategies for articular cartilage repair and regeneration. *Front Bioeng Biotechnol* 2021; 9: 770655.
8. Martín AR, Patel JM, Zlotnick HM, et al. Emerging therapies for cartilage regeneration in currently excluded 'red knee' populations. *NPJ Regen Med* 2019; 4: 12.
9. Petrigliano FA, Liu NQ, Lee S, et al. Long-term repair of porcine articular cartilage using cryopreservable, clinically compatible human embryonic stem cell-derived chondrocytes. *NPJ Regen Med* 2021; 6: 77.
10. Wang Y, Koole LH, Gao C, et al. The potential utility of hybrid photo-crosslinked hydrogels with non-immunogenic component for cartilage repair. *NPJ Regen Med* 2021; 6: 54.
11. Lee WYW and Wang B. Cartilage repair by mesenchymal stem cells: clinical trial update and perspectives. *J Orthop Translat* 2017; 9: 76–88.
12. Lam ATL, Reuveny S and Oh SKW. Human mesenchymal stem cell therapy for cartilage repair: review on isolation, expansion, and constructs. *Stem Cell Res* 2020; 44: 101738.
13. Le H, Xu W, Zhuang X, et al. Mesenchymal stem cells for cartilage regeneration. *J Tissue Eng* 2020; 11: 2041731420943839.
14. Sahu N, Budhiraja G and Subramanian A. Preconditioning of mesenchymal stromal cells with low-intensity ultrasound: influence on chondrogenesis and directed SOX9 signaling pathways. *Stem Cell Res Ther* 2020; 11: 1–15.
15. Mueller MB, Fischer M, Zellner J, et al. Hypertrophy in mesenchymal stem cell chondrogenesis: effect of TGF-beta isoforms and chondrogenic conditioning. *Cells Tissues Organs* 2010; 192: 158–166.
16. Futrega K, Robey PG, Klein TJ, et al. A single day of TGF-β1 exposure activates chondrogenic and hypertrophic differentiation pathways in bone marrow-derived stromal cells. *Commun Biol* 2021; 4: 29.
17. Lian C, Wang X, Qiu X, et al. Collagen type II suppresses articular chondrocyte hypertrophy and osteoarthritis progression by promoting integrin β1-SMAD1 interaction. *Bone Res* 2019; 7: 8.
18. Sun M, Chi G, Xu J, et al. Extracellular matrix stiffness controls osteogenic differentiation of mesenchymal stem cells mediated by integrin α5. *Stem Cell Res Ther* 2018; 9: 52.
19. Olivares-Navarrete R, Lee EM, Smith K, et al. Substrate stiffness controls osteoblastic and chondrocytic differentiation of mesenchymal stem cells without exogenous stimuli. *PLoS One* 2017; 12: e0170312.
20. Wu Y, Yang Z, Law JB, et al. The combined effect of substrate stiffness and surface topography on chondrogenic differentiation of mesenchymal stem cells. *Tissue Eng Part A* 2017; 23: 43–54.
21. Foyt DA, Taheem DK, Ferreira SA, et al. Hypoxia impacts human MSC response to substrate stiffness during chondrogenic differentiation. *Acta Biomater* 2019; 89: 73–83.
22. Mohammed M, Lai TS and Lin HC. Substrate stiffness and sequence dependent bioactive peptide hydrogels influence the chondrogenic differentiation of human mesenchymal stem cells. *J Mater Chem B* 2021; 9: 1676–1685.
23. Kim JS, Kim TH, Kang DL, et al. Chondrogenic differentiation of human ASCs by stiffness control in 3D fibrin hydrogel. *Biochem Biophys Res Commun* 2020; 522: 213–219.
24. Freeman FE, Schiavi J, Brennan MA, et al. Mimicking the biochemical and mechanical extracellular environment of the endochondral ossification process to enhance the in vitro mineralization potential of human mesenchymal stem cells. *Tissue Eng Part A* 2017; 23: 1466–1478.
25. Engler AJ, Sen S, Sweeney HL, et al. Matrix elasticity directs stem cell lineage specification. *Cell* 2006; 126: 677–689.
26. Petzold J and Gentleman E. Intrinsic mechanical cues and their impact on stem cells and embryogenesis. *Front Cell Dev Biol* 2021; 9: 761871.
27. Naqvi SM and McNamara LM. Stem cell mechanobiology and the role of biomaterials in governing mechanotransduction and matrix production for tissue regeneration. *Front Bioeng Biotechnol* 2020; 8: 597661.
28. Gattazzo F, Urciuolo A and Bonaldo P. Extracellular matrix: a dynamic microenvironment for stem cell niche. *Biochim Biophys Acta Gen Subj* 2014; 1840: 2506–2519.
29. Yang Y, Wang K, Gu X, et al. Biophysical Regulation of cell behavior-cross talk between substrate stiffness and nanotopography. *Engineering* 2017; 3: 36–54.
30. Pittenger MF, Discher DE, Péault BM, et al. Mesenchymal stem cell perspective: cell biology to clinical progress. *NPJ Regen Med* 2019; 4: 22.
31. Wan W, Cheng B, Zhang C, et al. Synergistic effect of matrix stiffness and inflammatory factors on osteogenic differentiation of MSC. *Biophys J* 2019; 117: 129–142.
32. Li J and Dong S. The signaling pathways involved in chondrocyte differentiation and hypertrophic differentiation. *Stem Cells Int* 2016; 2016: 2470351.
33. Wang T and Yang F. A comparative study of chondroitin sulfate and heparan sulfate for directing three-dimensional chondrogenesis of mesenchymal stem cells. *Stem Cell Res Ther* 2017; 8(1): 284.
34. Moulisová V, Poveda-Reyes S, Sanmartín-Masiá E, et al. Hybrid protein-glycosaminoglycan hydrogels promote chondrogenic stem cell differentiation. *ACS Omega* 2017; 2: 7609–7620.
35. Wang T, Lai JH and Yang F. Effects of hydrogel stiffness and extracellular compositions on modulating cartilage regeneration by mixed populations of stem cells and chondrocytes in vivo. *Tissue Eng Part A* 2016; 22: 1348–1356.
36. Zheng L, Liu S, Cheng X, et al. Intensified stiffness and photodynamic provocation in a collagen-based composite hydrogel drive chondrogenesis. *Adv Sci* 2019; 6(16): 1900099.
37. Galarraga JH, Locke RC, Witherel CE, et al. Fabrication of MSC-laden composites of hyaluronic acid hydrogels reinforced with MEW scaffolds for cartilage repair. *Biofabrication* 2022; 14: 014106.
38. Aprile P, Whelan IT, Sathy BN, et al. Soft hydrogel environments that facilitate cell spreading and aggregation preferentially support chondrogenesis of adult stem cells. *Macromol Biosci* 2022; 22: e2100365.
39. Jahanbakhsh A, Nourbakhsh MS, Bonakdar S, et al. Evaluation of alginate modification effect on cell-matrix interaction, mechanotransduction and chondrogenesis of encapsulated MSCs. *Cell Tissue Res* 2020; 381: 255–272.

40. Barceló X, Eichholz KF, Garcia O, et al. Tuning the degradation rate of alginate-based bioinks for bioprinting functional cartilage tissue. *Biomedicines* 2022; 10: 1621.
41. Ewa-Choy YW, Pingguan-Murphy B, Abdul-Ghani NA, et al. Effect of alginate concentration on chondrogenesis of co-cultured human adipose-derived stem cells and nasal chondrocytes: a biological study. *Biomater Res* 2017; 21: 19.
42. Liu W, Madry H and Cucchiarini M. Application of alginate hydrogels for next-generation articular cartilage regeneration. *Int J Mol Sci* 2022; 23: 1147.
43. Aprile P and Kelly DJ. Hydrostatic pressure regulates the volume, aggregation and chondrogenic differentiation of bone marrow derived stromal cells. *Front Bioeng Biotechnol* 2021; 8: 619914.
44. Abasalizadeh F, Moghaddam SV, Alizadeh E, et al. Erratum: alginate-based hydrogels as drug delivery vehicles in cancer treatment and their applications in wound dressing and 3D bioprinting (Journal of Biological Engineering (2020) 14: 8 DOI: 10.1186/s13036-020-0227-7). *J Biol Eng* 2020; 14: 1–22.
45. Xia H, Liang C, Luo P, et al. Pericellular collagen i coating for enhanced homing and chondrogenic differentiation of mesenchymal stem cells in direct intra-articular injection. *Stem Cell Res Ther* 2018; 9: 174.
46. Szychlinska MA, Calabrese G, Ravalli S, et al. Evaluation of a cell-free collagen type i-based scaffold for articular cartilage regeneration in an orthotopic rat model. *Materials* 2020; 13: 2369.
47. Rothdiener M, Hegemann M, Uynuk-Ool T, et al. Stretching human mesenchymal stromal cells on stiffness-customized collagen type I generates a smooth muscle marker profile without growth factor addition. *Sci Rep* 2016; 6: 35840.
48. Hu T and Lo ACY. Collagen-alginate composite hydrogel: Application in tissue engineering and biomedical sciences. *Polymers* 2021; 13: 1852.
49. Caliari SR and Burdick JA. A practical guide to hydrogels for cell culture. *Nat Methods* 2016; 13: 405–414.
50. Subramani R, Izquierdo-Alvarez A, Bhattacharya P, et al. The influence of swelling on elastic properties of polyacrylamide hydrogels. *Front Mater* 2020; 7: 1–13.
51. Ahearne M, Yang Y, El Haj AJ, et al. Characterizing the viscoelastic properties of thin hydrogel-based constructs for tissue engineering applications. *J R Soc Interface* 2005; 2: 455–463.
52. Civita P, M. Leite D and Pilkington GJ. Pre-clinical drug testing in 2d and 3d human in vitro models of glioblastoma incorporating non-neoplastic astrocytes: tunneling nano tubules and mitochondrial transfer modulates cell behavior and therapeutic respons. *Int J Mol Sci* 2019; 20: 6017.
53. Leite DM, Zvar Baskovic B, Civita P, et al. A human co-culture cell model incorporating microglia supports glioblastoma growth and migration, and confers resistance to cytotoxics. *FASEB J* 2020; 34: 1710–1727.
54. Di Luca A, Klein-Gunnewiek M, Vancso JG, et al. Covalent binding of bone morphogenetic protein-2 and transforming growth factor-β3 to 3D plotted scaffolds for osteochondral tissue regeneration. *Biotechnol J* 2017; 12: 1–9.
55. Di Luca A, Szlazak K, Lorenzo-Moldero I, et al. Influencing chondrogenic differentiation of human mesenchymal stromal cells in scaffolds displaying a structural gradient in pore size. *Acta Biomater* 2016; 36: 210–219.
56. Neves SC, Mota C, Longoni A, et al. Additive manufactured polymeric 3D scaffolds with tailored surface topography influence mesenchymal stromal cells activity. *Biofabrication* 2016; 8: 025012.
57. Huang S, Song X, Li T, et al. Pellet coculture of osteoarthritic chondrocytes and infrapatellar fat pad-derived mesenchymal stem cells with chitosan/hyaluronic acid nanoparticles promotes chondrogenic differentiation. *Stem Cell Res Ther* 2017; 8(1): 264.
58. Gale AL, Linardi RL, McClung G, et al. Comparison of the chondrogenic differentiation potential of equine synovial membrane-derived and bone marrow-derived mesenchymal stem cells. *Front Vet Sci* 2019; 6: 178.
59. Dikina AD, Almeida HV, Cao M, et al. Scaffolds derived from ECM produced by chondrogenically induced human MSC condensates support human MSC chondrogenesis. *ACS Biomater Sci Eng* 2017; 3: 1426–1436.
60. Sarem M, Otto O, Tanaka S, et al. Cell number in mesenchymal stem cell aggregates dictates cell stiffness and chondrogenesis. *Stem Cell Res Ther* 2019; 10: 10.
61. Park JS, Chu JS, Tsou AD, et al. The effect of matrix stiffness on the differentiation of mesenchymal stem cells in response to TGF-β. *Biomaterials* 2012; 32: 3921–3930.
62. Kilian KA, Bugarija B, Lahn BT, et al. Geometric cues for directing the differentiation of mesenchymal stem cells. *Proc Natl Acad Sci U S A* 2010; 107: 4872–4877.
63. McCorry MC, Puetzer JL and Bonassar LJ. Characterization of mesenchymal stem cells and fibrochondrocytes in three-dimensional co-culture: analysis of cell shape, matrix production, and mechanical performance. *Stem Cell Res Ther* 2016; 7(1): 39.
64. Heng BC, Zhang X, Aubel D, et al. Role of YAP/TAZ in cell lineage fate determination and related signaling pathways. *Front Cell Dev Biol* 2020; 8: 735.
65. Kovar H, Bierbaumer L and Radic-Sarikas B. The YAP/TAZ Pathway in osteogenesis and bone sarcoma pathogenesis. *Cells* 2020; 9: 1–34.
66. Hwang JH, Byun MR, Kim AR, et al. Extracellular matrix stiffness regulates osteogenic differentiation through MAPK activation. *PLoS One* 2015; 10: e0135519.
67. Barcelona-Estaje E, Dalby MJ, Cantini M, et al. You Talking to me? Cadherin and integrin crosstalk in biomaterial design. *Adv Healthc Mater* 2021; 10: e2002048.
68. Goude MC, McDevitt TC and Temenoff JS. Chondroitin sulfate microparticles modulate transforming growth factor-β1-induced chondrogenesis of human mesenchymal stem cell spheroids. *Cells Tissues Organs* 2014; 199: 117–130.
69. Sun AX, Lin H, Fritch MR, et al. Chondrogenesis of human bone marrow mesenchymal stem cells in 3-dimensional, photocrosslinked hydrogel constructs: Effect of cell seeding density and material stiffness. *Acta Biomater* 2017; 58: 302–311.
70. Saha A, Rolfe R, Carroll S, et al. Chondrogenesis of embryonic limb bud cells in micromass culture progresses rapidly to hypertrophy and is modulated by hydrostatic pressure. *Cell Tissue Res* 2017; 368: 47–59.
71. Carroll SF, Buckley CT and Kelly DJ. Cyclic hydrostatic pressure promotes a stable cartilage phenotype and enhances

the functional development of cartilaginous grafts engineered using multipotent stromal cells isolated from bone marrow and infrapatellar fat pad. *J Biomech* 2014; 47: 2115–2121.
72. Pattappa G, Johnstone B, Zellner J, et al. The importance of physioxia in mesenchymal stem cell chondrogenesis and the mechanisms controlling its response. *Int J Mol Sci* 2019; 20: E484.
73. Sathy BN, Daly A, Gonzalez-Fernandez T, et al. Hypoxia mimicking hydrogels to regulate the fate of transplanted stem cells. *Acta Biomater* 2019; 88: 314–324.
74. Hwang OK, Noh YW, Hong JT, et al. Hypoxia pretreatment promotes chondrocyte differentiation of human adipose-derived stem cells via vascular endothelial growth factor. *Tissue Eng Regen Med* 2020; 17: 335–350.
75. Schmidt S, Abinzano F, Mensinga A, et al. Differential production of cartilage ECM in 3D agarose constructs by equine articular cartilage progenitor cells and mesenchymal stromal cells. *Int J Mol Sci* 2020; 21(19): 1.
76. Hu X, Yu SP, Fraser JL, et al. Transplantation of hypoxia-preconditioned mesenchymal stem cells improves infarcted heart function via enhanced survival of implanted cells and angiogenesis. *J Thorac Cardiovasc Surg* 2008; 135: 799–808.
77. Elabd C, Ichim TE, Miller K, et al. Comparing atmospheric and hypoxic cultured mesenchymal stem cell transcriptome: implication for stem cell therapies targeting intervertebral discs. *J Transl Med* 2018; 16: 222.
78. Tamaddon M, Blunn G, Xu W, et al. Sheep condyle model evaluation of bone marrow cell concentrate combined with a scaffold for repair of large osteochondral defects. *Bone Jt Res* 2021; 10: 677–689.
79. Moran CJ, Ramesh A, Brama PA, et al. The benefits and limitations of animal models for translational research in cartilage repair. *J Exp Orthop* 2016; 3: 1–12.
80. Lydon H, Getgood A and Henson FMD. Healing of osteochondral defects via endochondral ossification in an Ovine model. *Cartilage* 2019; 10: 94–101.
81. Kresakova L, Danko J, Vdoviakova K, et al. In vivo study of osteochondral defect regeneration using innovative composite calcium phosphate biocement in a sheep model. *Materials* 2021; 14: 4471.
82. Haddouti EM, Randau TM, Hilgers C, et al. Characterization and comparison of human and ovine mesenchymal stromal cells from three corresponding sources. *Int J Mol Sci* 2020; 21: E2310.
83. Sanjurjo-Rodríguez C, Castro-Viñuelas R, Hermida-Gómez T, et al. Ovine mesenchymal stromal cells: morphologic, phenotypic and functional characterization for osteochondral tissue engineering. *PLoS One* 2017; 12: e0171231.
84. Khan MR, Chandrashekran A, Smith RKW, et al. Immunophenotypic characterization of ovine mesenchymal stem cells. *Cytometry A* 2016; 89: 443–450.